Shortwave Direction and Spreading Measured with HF Radar

LUCY R. WYATT

School of Mathematics and Statistics, University of Sheffield, and Seaview Sensing, Ltd., Sheffield Technology Parks, Sheffield, United Kingdom

(Manuscript received 25 May 2011, in final form 10 August 2011)

ABSTRACT

The accuracy of wave direction and spreading at the Bragg-matched wavelength measured with HF radar over a wide range of HF operating frequencies is demonstrated by comparison with buoy data. The agreement for shortwave direction is better than that obtained for wind direction, which has been the more common application of this measurement, because these waves are not always aligned with the wind direction, particularly in short fetch and low wind speed situations. The method assumes a model of shortwave directionality and the validity of this is explored by using the buoy Fourier coefficients, with inconclusive results. The radar measurements do not use the linear dispersion relationship, but the comparison with buoy data does, and the implications of this are discussed.

1. Introduction

HF radars measure backscatter from the ocean surface over an area from the coast to a maximum range determined by the radar design, operating frequency, wave height, external noise, and interference levels. The backscatter is converted to surface current speed and direction (Stewart and Joy 1974; Barrick et al. 1977; Robinson et al. 2011), significant wave height (Barrick 1977; Maresca and Georges 1980; Wyatt 1988, 2002; Graber and Heron 1997; Gurgel et al. 2006), the ocean wave directional spectrum (Lipa 1977; Lipa and Barrick 1986; Wyatt 1990, 2000; Howell and Walsh 1993, Hisaki 1996; Hashimoto and Tokuda 1999; Green and Wyatt 2006), and wind speed and direction (Long and Trizna 1973; Dexter and Theodorides 1982; Georges et al. 1993; Wyatt et al. 1997; Vesecky et al. 2002) for all of the data of suitable quality with sufficient signal-to-noise.

All of these measurements are made using the radar backscatter power spectrum (usually referred to as the Doppler spectrum), which is normally dominated by two peaks resulting from Bragg scatter from linear ocean waves with half the radio wavelength (Barrick 1972), that is, with the wavenumber given by $k_{sw} = 4\pi g F_r/300$, where F_r is the operating frequency of the radar and g is gravity. If the linear wave dispersion relationship in deep water is assumed, then the frequency of these waves is given by $f_{sw} = (1/2\pi)\sqrt{4\pi g F_r/300}$ (a modification for finite-depth water is straightforward). Wind direction estimates are made by looking at the ratio of these two first-order Bragg peaks and fitting a wave model to this on the assumption that these short waves are wind driven and aligned with the wind. Such wave models normally have two parameters—direction and directional spreading. A single radar provides just one measurement, the Bragg ratio, and hence only one of these parameters, usually wind direction, can be estimated. This has a directional ambiguity in that it is not possible to distinguish between wind direction to the right of the radar beam and that to the left. Tyler et al. (1974), Stewart and Barnum (1975), and Heron et al. (1985) did include variable directional spreading in their estimation of wind direction from the Bragg peaks, but obtained this using external information. Heron (1987) extracted both direction and spreading using data from the same radar but on different beams. Bragg ratio measurements from two radars looking in different directions at the same area of sea make it possible to measure both parameters of the directional distribution without making assumptions about spatial homogeneity.

Wyatt et al. (1997) presented a maximum-likelihood (WLA) method to estimate the directional distribution of these short ocean waves. The original method was

Corresponding author address: Lucy R. Wyatt, School of Mathematics and Statistics, University of Sheffield, Sheffield S3 7RH, United Kingdom.
E-mail: wyatt@sheffield.ac.uk

DOI: 10.1175/JTECH-D-11-00096.1

© 2012 American Meteorological Society

applied to data collected with the Ocean Surface Current Radar (OSCR) HF radar operating in the range of 25–27 MHz for which the short waves have frequencies of 0.51–0.53 Hz, which are very likely to be aligned with the wind, except in very calm conditions. Since then a lot of HF radars have operated at lower radio frequencies in order to increase range. For these, some care has to be taken in the interpretation of these directions. They are still indicating the direction of the Bragg-matched ocean waves, but in low winds or in fetch-limited conditions these waves may not be wind driven. In Wyatt et al. (2006) the estimated wind directions were filtered to exclude those for which the ratio of the Bragg frequency to the maximum frequency in a Pierson–Moskowitz spectrum (using the Met Office wave model wind speeds, which were made available for that deployment) was less than one, and good agreement with model wind directions was obtained.

Hisaki (2004) considered the possibility that the distribution of energy at the Bragg-matched wavelength may be bimodal, as suggested by other authors (e.g., Ewans 1998; Young 2010; Toffoli et al. 2010), based on wave model and measured data. These authors describe the development of bimodality at frequencies away from the wave spectral peak, and this has been attributed to wave–wave interactions by Longuet-Higgins (1976) and Banner and Young (1994). Hisaki (2002) used a similar method to that of WLM, and in Hisaki (2004, 2007) a double-$\cos^{2s}$ model was fitted to his radar data. Although this model appeared to fit the data better than a single-mode model when it was assessed using Akaike's information criterion (Akaike 1974), bimodality was only present in the case when shortwave directions were shifting in response to the wind. For most cases the double-$\cos^{2s}$ model provided only a different shape for a unimodal model. Similar cases of shortwave bimodality in association with changing wind fields were discussed in Wyatt (1999) and Hauser et al. (2005, hereafter HI).

Young (2010) discussed the directional spreading for waves measured with a high-resolution spatial array in Lake George. He presented the intriguing result that while bimodality was evident in the wavenumber spectra it was not seen in the frequency spectra. By looking at the wavenumber–frequency spectrum using wavelet methods, he showed that waves roughly in the direction of the wind and away from the spectral peak did not appear to follow the linear dispersion relationship, whereas those at more off-wind directions did. He suggested that this could be explained by the Doppler shifting of the shorter waves by the longer waves near the peak, thus elevating spectral levels in the directional frequency spectrum in the wind direction and masking any bimodality. Ewans (1998), on the other hand, did appear to find bimodality in buoy-measured directional frequency spectra in fetch-limited seas.

The issue of the validity of the linear dispersion relationship at wavenumbers/frequencies beyond the spectral peak has been considered by a number of authors. As pointed out by LeBlond (1986) and Barrick (1986), this is particularly important for HF radar because the linear dispersion relationship is used in the estimation of surface currents. Barrick (1986) argued that the dispersion relationship does hold in this case because the radar is measuring the wavenumber-frequency spectrum at the Bragg matched wavelength and the peak of this corresponds to the linear dispersion relationship. Phillips (1981) provided a related argument to demonstrate that the dispersion relationship does hold if the measurement system can isolate the short waves in both space and time. The array used by Young should have this property and yet he provides evidence that the dispersion relationship does not hold in some parts of the spectrum. This will be discussed further in section 4 below.

In the next section of this paper we summarize the WLA method and then, in the following section, apply it to data from a number of different radar deployments at different radio frequencies, focusing in particular on the value of the estimate as a wave, rather than wind direction, measurement. A discussion of the wave model used, bimodality, and the validity of the linear dispersion relationship using these datasets is explored in section 4, followed by concluding remarks.

2. WLA method

The WLA method has been described in Wyatt et al. (1997). It adopts the same approach as others who have developed wind direction algorithms by looking at the ratio of the two first-order Bragg peaks and fitting a wave model to this. A two-parameter model is used to describe mean propagation direction and the spreading of energy about this, and a maximum likelihood estimator is used. The Donelan et al. (1985) spreading model is used, that is, $\mathrm{sech}^2\,\beta(\theta - \theta_w)$, where β is related to the directional spreading and θ_w is the wave direction. This has the advantage over the $\cos^{2s}$ model that is usually adopted (by Hisaki 2002, e.g.), in that it can model energy propagating against the mean direction, which is consistent with the observation of two first-order Bragg peaks in all cases. An alternative spreading function in the form of a Gaussian has been proposed by Apel (1994) and used by Haus et al. (2010), but the differences from the sech model are small, so this form has not been considered here. The unified spreading model proposed by Elfouhaily et al. (1997) has not been used here either for similar reasons.

Denoting r' as the measured Bragg ratio and r as the modeled Bragg ratio, the method requires the maximization of the probability density function of the measured Bragg ratio, which can be written as

$$\frac{\frac{1}{2}\Gamma(\nu)\left(\frac{r'}{r}\right)^{(\nu/2-1)}}{\left[\Gamma\left(\frac{\nu}{2}\right)\right]^2\left(1+\frac{r'}{r}\right)^{\nu}},$$

where ν is the degrees of freedom of the Doppler spectral estimates.

To improve the robustness of the estimate, data from $n-1$ neighboring measurement cells (where n is normally 9) are combined with the data at the selected cell, giving a probability distribution function (PDF) to maximize of

$$\prod_{i=1}^{n}\frac{\frac{1}{2}\Gamma(\nu)\left(\frac{r'}{r}\right)^{(\nu/2-1)}}{\left[\Gamma\left(\frac{\nu}{2}\right)\right]^2\left(1+\frac{r'}{r}\right)^{\nu}}.$$

This can be written as follows:

$$\left[\frac{\Gamma(\nu)}{\Gamma(\nu/2)^2}\right]^n\left[\prod_{i=1}^{n}(r_i')^{\nu/2-1}\right]\left[\prod_{i=1}^{n}\frac{r_i}{(r_i+r_i')^2}\right]^{\nu/2}.$$

The first two terms do not depend on the parameters that we are seeking to estimate, and so we only need to consider the third term in the maximization. Because $\nu > 0$, the problem reduces to maximizing

$$\prod_{i=1}^{n}\frac{r_i}{(r_i+r_i')^2},$$

or, equivalently,

$$\sum_{i=1}^{n}\ln\left[\frac{r_i}{(r_i+r_i')^2}\right].$$

For the Donelan et al. (1985) model the maximization provides estimates of β and θ_w, the shortwave direction at the first-order Bragg-matched ocean wavenumber. Because this wavenumber is usually high compared to the spectral peak, this direction is also used as an estimate of wind direction although, as mentioned above, with lower accuracy in low sea and fetch-limited conditions.

3. Comparisons with buoy measurements

Data from three different experiments are used here to demonstrate the accuracy of the radar measurements. In all cases an industry-standard Datawell Directional Waverider was deployed to provide directional wave data for validation.

During the European Union (EU)-funded European Radar Ocean Sensing (EuroROSE) project (Wyatt et al. 2003) a Wave Radar (WERA) HF radar system (Gurgel et al. 1999) was deployed on the west coast of Norway on the islands of Fedje and Lyngoy, providing data for shipping coming into the oil terminals on the mainland. These operated at ~27 MHz and collected data for more than 1 month during February–April 2000. An anemometer located on the island of Hellisoy provided wind data and a Directional Waverider buoy was located about 10 km offshore for wave measurement validation.

The Pisces HF radar system (Wyatt et al. 2006) was deployed at sites in Devon and South Wales in the United Kingdom from December 2003 to June 2006, collecting data to demonstrate radar wave measurement accuracy. A Directional Waverider was located 60 km offshore. Wind data were not available, but the Met Office provided model winds used to drive their wave model.

The final dataset is taken from a 4-month period (November 2005–February 2006) of WERA data collected in Liverpool Bay by the Proudman Oceanographic Laboratory [now the National Oceanography Centre, Southampton (NOC)]. This installation is part of the NOC Coastal Observatory (Howarth et al. 2007). Again a Directional Waverider is deployed within the radar look area, and an anemometer is located at the Dee Estuary to the south of the coverage area. These data are all available for download from the Coastal Observatory website.

Data from all three deployments can be seen and downloaded from the Seaview Sensing website. Details about the experimental setups are summarized in Table 1.

Figure 1 shows the time series of wave direction and directional spreading for the three datasets shown in order of increasing radar frequency. Subsets of the Celtic Sea and Liverpool Bay data are used here for clarity. Directions are those toward which the waves are propagating. The figures show generally good agreement. The directional spreading σ, shown here, is determined from β for the case of the radar data using $\sigma = \sqrt{2(1-r)}(180/\pi)$, where $r = (\pi/2\beta)/\sinh(\pi/2\beta)$ (HI). It can be interpreted as the half-width, and thus the direction $\pm\sigma$ is plotted in the figures. The direction comparisons are presented as scatterplots in Fig. 2 and statistics of the comparison are shown in Table 2. In the table the wind direction comparisons are also included to demonstrate that the accuracy is greater when considered as wave directions, although it should be noted that in none of these cases were there collocated wind direction measurements.

TABLE 1. Summary of experimental configurations. Directions (°) are clockwise from the north.

Location	Celtic Sea	Liverpool Bay	Fedje, Norway
Radar	Pisces	WERA	WERA
Operating frequency	7–10 MHz	13 MHz	27 MHz
Depth at buoy location (m)	68	22	280
Range from radars to buoy location (km)	60, 59	32, 18	10, 8
Direction from radars to buoy location	−70, −159	33, −93	−141, −64
Source of wind data	Met Office model	Coastal anemometer	Coastal anemometer
Average wind speed ($m\ s^{-1}$)	9.5	7.9	7.1
Limited fetch wind directions (from)	West–northwest and north–east–south, exposed to the Atlantic to the southwest and the Irish Sea to the north	East–south, with a longer fetch from the west	North-northeast–east–south-southeast

The comparisons for the Celtic Sea and Liverpool Bay datasets are better than those reported by Hisaki (2007), and those from Norway are similar. Hisaki was making comparison with model data, whereas here the comparison is with buoy data. In addition, the radar data used here are probably of better quality in general. In Hisaki (2004), it is noted that for their radar data the signal-to-noise was only sufficient for first-order scattering, whereas the data used here have also been used for wave measurement, which uses the second-order part of the spectrum (Wyatt et al. 2011). It is difficult to draw any firm conclusions about the relative accuracy between these three experiments because there is no in situ wind data for any of them.

The buoy measurements included in these comparisons are at the Bragg-matched frequency and the comparisons suggest that there is more temporal variability in these for the higher-frequency comparison shown in Fig. 1c. This is less evident in the radar measurements.

In Fig. 1 the directional spreading parameter β was converted to an angular spread. Although the comparison with the buoy looks reasonable in this figure, there is a lot of scatter, as reflected in the correlation coefficients in Table 2. For the cases where wind sea dominates the spectrum, the radar measurements of β can be compared with empirical values obtained by Donelan et al. (1985). In Fig. 3, the β measured by the radar is plotted as a function of wave (Bragg) frequency normalized by the buoy peak frequency in the wind wave part of the spectrum. This peak has been identified from the buoy spectral data using the method for partitioning buoy spectra proposed by Voorrips et al. (1997), with some small modifications to improve the reliability with these datasets. The modifications were as follows: 1) a threshold on the null between two neighboring maxima was increased from 50% to 70%; 2) the minimum energy for a separate partition was selected to be 5% of the maximum partition energy for that spectrum; 3) peak directions between neighboring partitions were compared, and the difference that would prevent merging was raised from 50° to 70°; and 4) peak rather than mean directions have been used in the application of the Voorrips et al. wind sea criterion (note that this accounts for slanting fetch). In addition, any data for which the peak energy density in the wind wave partition obtained from this process is less than twice that in any other partition is excluded from further analysis. Thus, strong swell events are excluded. We note that Ardhuin et al. (2007) have suggested that moderate swell does not affect the wind sea part of the spectrum, but it is not the intention in this paper to explore swell impacts, so we have restricted the discussion predominantly to wind seas (within the limitations of the partitioning process). Note that there is no evidence in the cases that emerge from this analysis that there is any significant difference between the wind wave peak direction and the direction at the Bragg peak, as might have occurred if there were significant slanting fetch or current shear, for example (Zhang et al. 2009). For the Norway dataset in particular, large amounts of data were removed from consideration as a result of the partitioning. The use of the onshore wind speeds may have eliminated a number of wind sea cases associated with higher offshore winds from this dataset.

The dashed line in Fig. 3 shows the dependence of β on wave (Bragg) frequency normalized by the buoy spectral peak frequency, as proposed by Donelan et al. (1985). Also shown is the additional decay in β at higher frequencies proposed by Banner (1990). It can be seen that for the Norwegian dataset at 27 MHz, the Bragg frequencies were always well away from the Bragg peak, whereas a significant portion of the Liverpool and

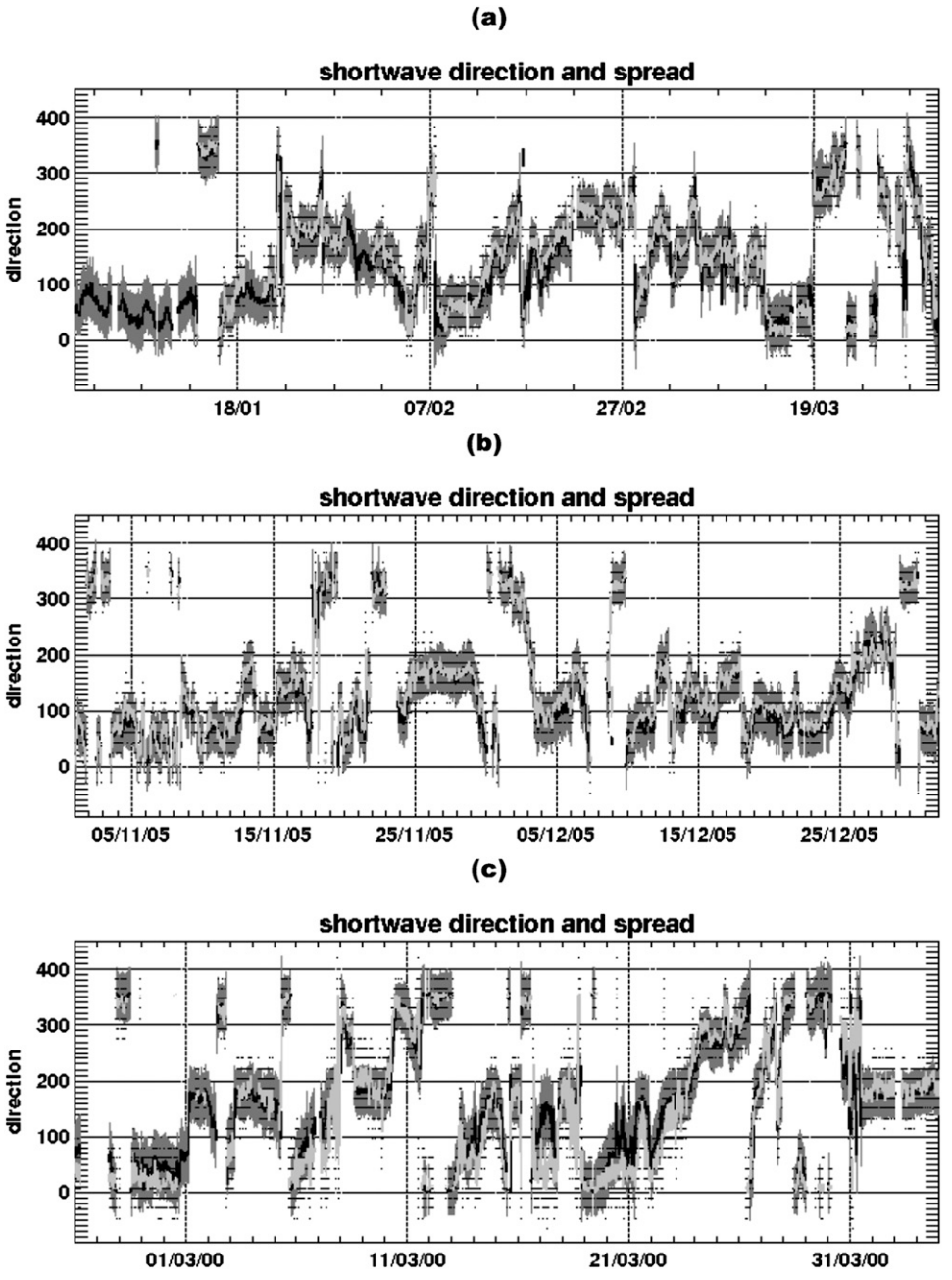

FIG. 1. Comparisons of radar wave direction (black line) and spreading (dark gray shading) with the corresponding buoy measurements at the Bragg-matched ocean wave frequency, direction (light gray line), and spread (dashed). (a) Celtic Sea, (b) Liverpool Bay, and (c) Fedje.

Celtic Sea datasets contain wave spectra with the spectral peak close to the Bragg peak. In the case of Liverpool Bay there are examples where the Bragg peak is below the peak frequency. In these two cases there is no evidence that the radar measurements follow the Donelan et al. form for lower frequencies. In all cases the radar measurements lie between the Donelan et al. and Banner formulations away from the spectral peak.

To compare the buoy and radar data with other directional spreading models, both measurements of directional spreading have been converted to the s parameter using $s = 1 - (\sigma^2/2)$ (Tucker and Pitt 2001). This comparison is shown in Fig. 4, again as a function of the Bragg-to-peak buoy frequency. Shown on here are the directional spreading models for fully developed seas of Mitsuyasu et al. (1975), Hasslemann et al. (1980), and Ewans (1998).

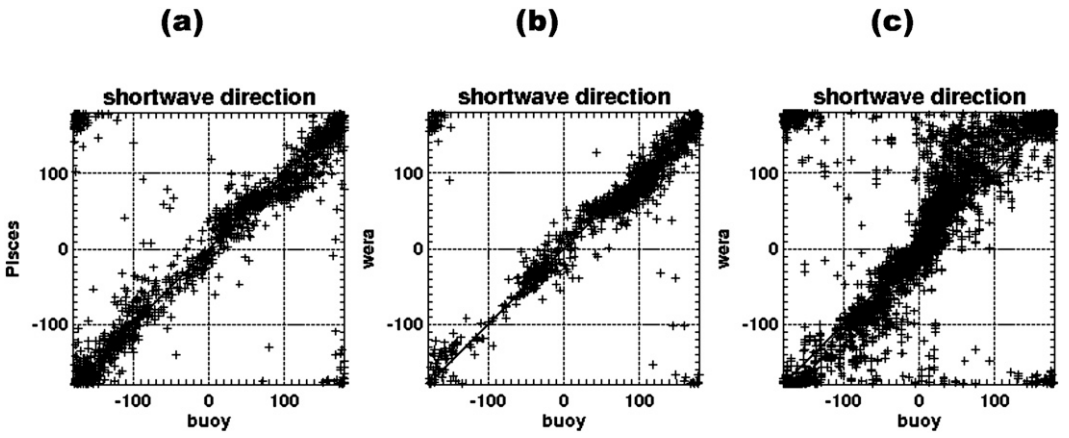

FIG. 2. Scatterplots of shortwave directions for (a) Celtic Sea, (b) Liverpool Bay, and (c) Fedje.

While the buoy data do show evidence of increasing s near to the spectral peak, this is not seen in the radar data and there is significant variability in both measurements. Both the Mitsuyasu et al. and Hasselman et al. models include a wave age dependence (see, e.g., Ewans 1998 for a discussion). Wave age U/c_p is estimated using the available wind speed U and the phase speed c_p at the peak of the buoy wind wave spectrum. Figure 5 shows the Liverpool Bay data in Fig. 4 for five wave age bands together with the Mitsuyasu et al. and Hasselman et al. models for the extremes of these bands. The Mitsuyasu et al. model predicts much large changes in s with wave age over the ranges in this dataset than can be seen in either the buoy or radar data. The Hassleman et al. model predicts small changes beyond the peak, but the data in this region are mostly above this curve. There is little evidence in the data of any wave age dependence, although of course this may be due to the limitations of the wind speed and peak frequency estimates. The same analysis has been done for the Celtic Sea and Norway data with similar inconclusive results.

4. Validity of the assumptions

a. The shortwave model

The method has assumed a Donelan et al. (1985) directional model for short ocean waves. Others have used a $\cos^{2s}$ model or, in the case of Hisaki (2004), a double-$\cos^{2s}$ model. As noted above neither the buoy nor the radar data are completely consistent with these models when assessed by their spreading parameters. We can also use the buoy data for these experiments at the Bragg frequency in other ways to see whether they are consistent with any of these models. In part I, section 2.5 of HI (hereafter HI, part I), relationships between the four Fourier coefficients provided by Directional Waveriders, a_i, b_i for $i = 1, 2$ expressed in terms of $r_i = \sqrt{a_i^2 + b_i^2}$, for a variety of directional models are given. Figure 6 shows the relationship between $\sqrt{r_2}$ and r_1 for the sech and $\cos^{2s}$ models and for the buoy data at the Bragg-matched frequency for the Celtic Sea and Norwegian datasets (a_2, b_2 were not available for the Liverpool Bay dataset). Also shown on these plots are the upper (dashed–dotted) and lower (dashed) bounds for unimodal symmetric distributions of which the Poisson, sech, and $\cos^{2s}$ are examples. Few of the data points fall outside these bounds, although it is not appropriate to conclude that this means there is no evidence for bimodality (HI, part I). Note that there can be no waves with Fourier coefficients that fall in the region to the right of the dotted line. The data have been separated into groups, indicated by different symbols on the plots, according to the ratio of the Bragg f_b to buoy-measured peak frequency f_p (after partitioning, as

TABLE 2. Comparison of radar r and in situ b, wave θ_{wv}, and wind θ_{wd} measurements; "N" is the number of compared measurements, and "cc" is the circular correlation coefficient.

Bragg frequency (Hz)	Pisces–Celtic Sea			WERA–Liverpool Bay			WERA–Norway		
	0.27–0.35			0.35–0.37			0.53		
Statistic	θ_{wv}	θ_{wd}	σ	θ_{wv}	θ_{wd}	σ	θ_{wv}	θ_{wd}	σ
N	1534	166	1534	1286	1286	1286	4783	774	4783
$\overline{r-b}$	−3.52°	−6.73°	2.95°	−7.04°	11.7°	1.73°	5.74°	7.42°	−4.58°
rms$(r-b)$	23.81°	32.12°	8.44°	20.26°	47.98°	8.94°	38.36°	39.2°	10.18°
cc	0.86	0.77	0.53	0.91	0.58	0.37	0.7	0.68	0.56

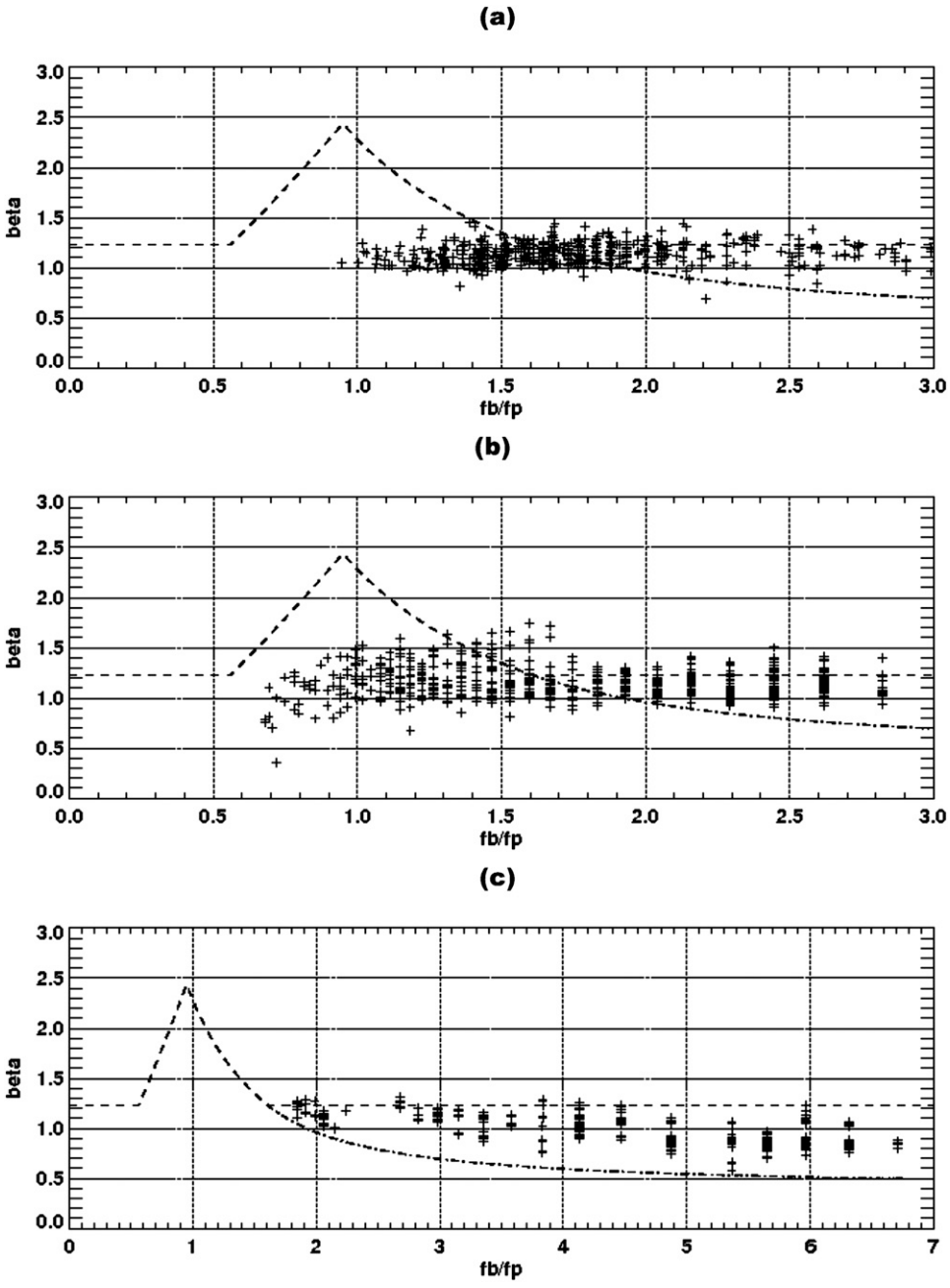

FIG. 3. The parameter β measured at the Bragg frequency compared with the Bragg-to-peak frequency ratio at the (a) Celtic Sea, (b) Liverpool Bay, and (c) Fedje. The Donelan et al. (1985) empirical curve (dashed line) and the Banner (1990) high-frequency extension (dash–dot line) are shown.

described in section 3). The few cases that are not consistent with a unimodal, symmetric distribution are for $f_b/f_p > 2.0$. The rest of the Celtic Sea data are mostly scattered between the Poisson distribution and the lower limit, with some indication that they behave more like the sech distribution at high r_1 and the $\cos^{2s}$ at lower r_1, but the results do not conclusively support either form. The Norway data are more scattered across the unimodal symmetric area with no evidence of preference for any particular form.

The discussion here is about directional bimodality at a particular frequency or range of frequencies, and not frequency bimodality, which is usually associated with mixed swell and wind sea, which is much easier to identify and understand. Most wave measurements are made with directional wave buoys, which provide only a limited

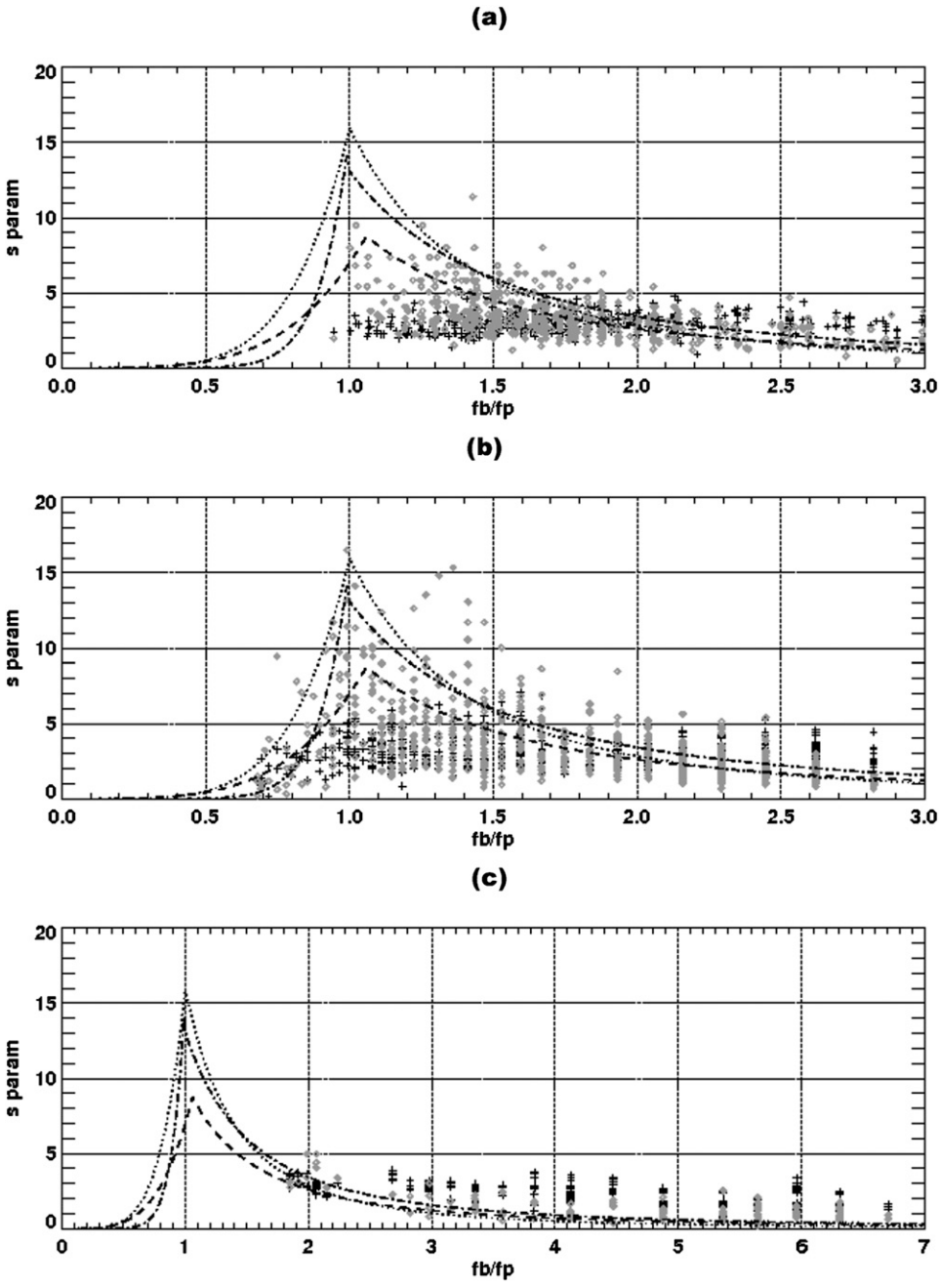

FIG. 4. The parameter *s* measured at the Bragg frequency compared with the Bragg-to-peak frequency ratio at the (a) Celtic Sea, (b) Liverpool Bay, and (c) Fedje. Radar (black +s) and buoy (gray ×s) data are shown. The Mitsuyasu et al. (1975) empirical curve (dotted line), Hasselmann et al. (1980) data (dashed line), and Ewans (1998) data (dash–dot line) are shown.

number of Fourier coefficients of the directional spectrum, and, thus, while some limits to possible unidirectional distributions can be asserted (as above), directional bimodality is difficult to identify. In recent years authors have used maximum likelihood (Benoit et al. 1997) or maximum entropy (Lygre and Krogstad 1986) methods to estimate the directional spectrum from these coefficients. In part II, section 5.3 of HI (hereafter HI, part II), such spectra are compared with HF radar data, but the evidence for bimodality is not completely consistent; that is, in some cases both buoy and radar show bimodality, but in other cases this is only evident in the

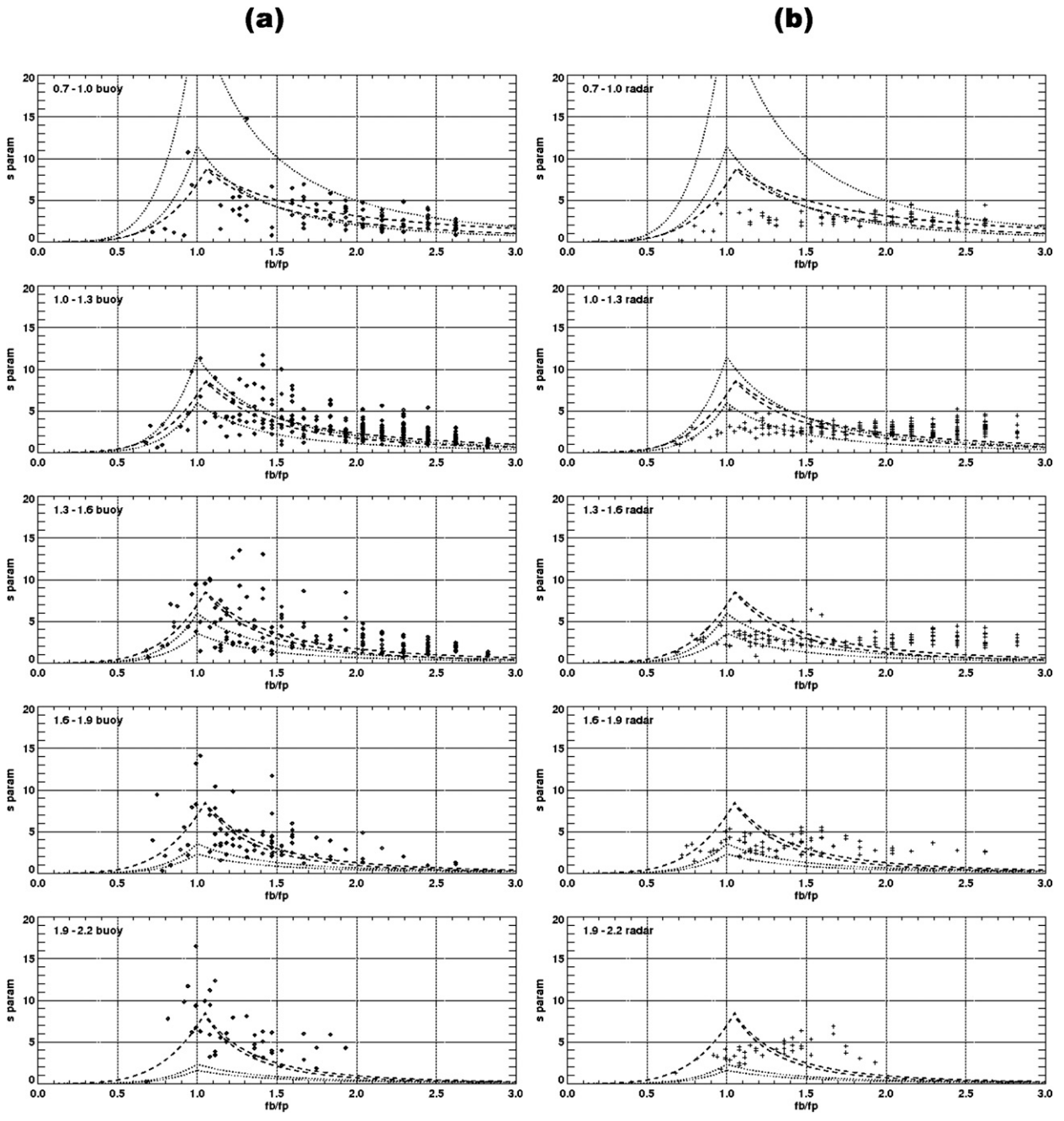

FIG. 5. The Liverpool Bay parameter *s* segregated by the wave age bands are shown (top left) for the (a) buoy and (b) radar. Upper and lower bounds for each band of the Mitsuyasu et al. (1975) empirical curve (dotted line), and Hasselmann et al. (1980) data (dashed line) are shown.

maximum entropy buoy spectra. Another method that makes use of the Fourier coefficients to indicate bimodality was suggested by Kuik et al. (1988), in this case using the skewness and kurtosis derived from the Fourier coefficients. Although it was suggested in HI, part I, that these are difficult to interpret and unstable in estimation, there is some evidence that they can indicate bimodality in HI, part II. This method was also applied by Ewans (1998) to demonstrate that most of his data were consistent with nonunimodal–symmetric distributions away from the peak frequency. Figure 7 shows the same dataset as that in Fig. 6, but plotted in terms of kurtosis and skewness. Rather more cases fall into the multimodal–nonsymmetric class than was the case with the r_i analysis,

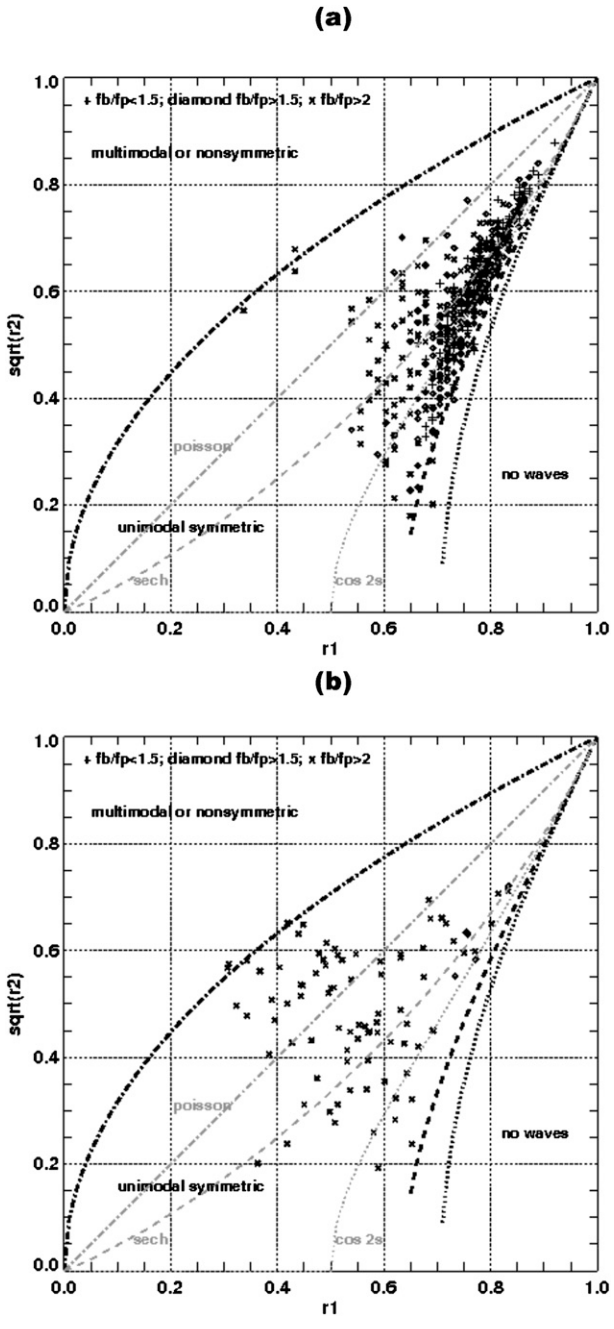

FIG. 6. Fourier coefficient relationships for the (a) Celtic Sea and (b) Fedje. The upper (dashed–dotted line) and lower (dashed line) bounds for unimodal symmetric distributions, and the lower bound for any waves (dotted line) are shown.

although the majority of the data are still consistent with unimodal, symmetric distributions. In the Celtic Sea case more of the potentially multimodal cases are for frequencies near the spectral peak, which may be indicating that swell was not completely removed by the partitioning process, perhaps because the swell and wind sea overlap in frequency at their extremes.

Of course the buoy data are frequency spectra and Young's (2010) data only show bimodality in the wavenumber spectrum, so it is still possible that a bimodal model should be used for the HF radar analysis, as was done by Hisaki (2004), because this is looking for the directional distribution at a particular wavenumber—twice the radio wavenumber—rather than a particular frequency.

b. Dispersion relationship

The estimation of shortwave direction does not depend on the dispersion relationship, but the comparisons with buoy data shown in section 3 do because they attribute the shortwave direction to a particular frequency. Barrick (1986) pointed out that if short waves were not governed by the dispersion relationship and were instead, as had been suggested, waves bound to the peak of the spectrum, then significant errors would have been identified in HF radar surface current measurements. There was already much evidence that this was not the case, and a large number of validation studies have been undertaken since then [see Robinson et al. (2011) for a summary of some of these], with no evidence of any problems. Nonetheless, Young (2010) does seem to show some evidence of a departure from the dispersion relationship in directions that are roughly aligned with the wind direction. The radar often uses information from both first-order peaks to estimate surface current. These correspond to Bragg waves propagating both toward and away from the radar site. Young's analysis suggests that as long as we are not looking roughly along the peak wave direction then the dispersion relationship will hold. When the radar looks into the peak wave direction the analysis suggests that the Bragg wave approaching the radar will be shifted to a higher frequency, but there is no discussion therein on the impact on the Bragg wave receding from the radar, and thus opposing the peak wave direction; although, if this is a result of Doppler shifting by the dominant waves, then one would expect it to be shifted to a lower frequency by a similar amount. The net result should be no change in the difference in frequency between the two Bragg peaks, that is, this Doppler shift appears to influence the radar spectrum in exactly the same way as a surface current. This would make it very difficult to use HF radar to separate a departure from the dispersion relationship from a wind-driven current. The frequency difference between the two peaks (expressed as a percentage difference from the difference that would be predicted with the linear dispersion relationship) as a function of both wind direction (from the radar look direction) and f_b/f_p have been examined. Figure 8 shows the variation with f_b/f_p, and in the Fedje case there is some evidence of a departure from the dispersion relationship for larger values of f_b/f_p, although not for all cases.

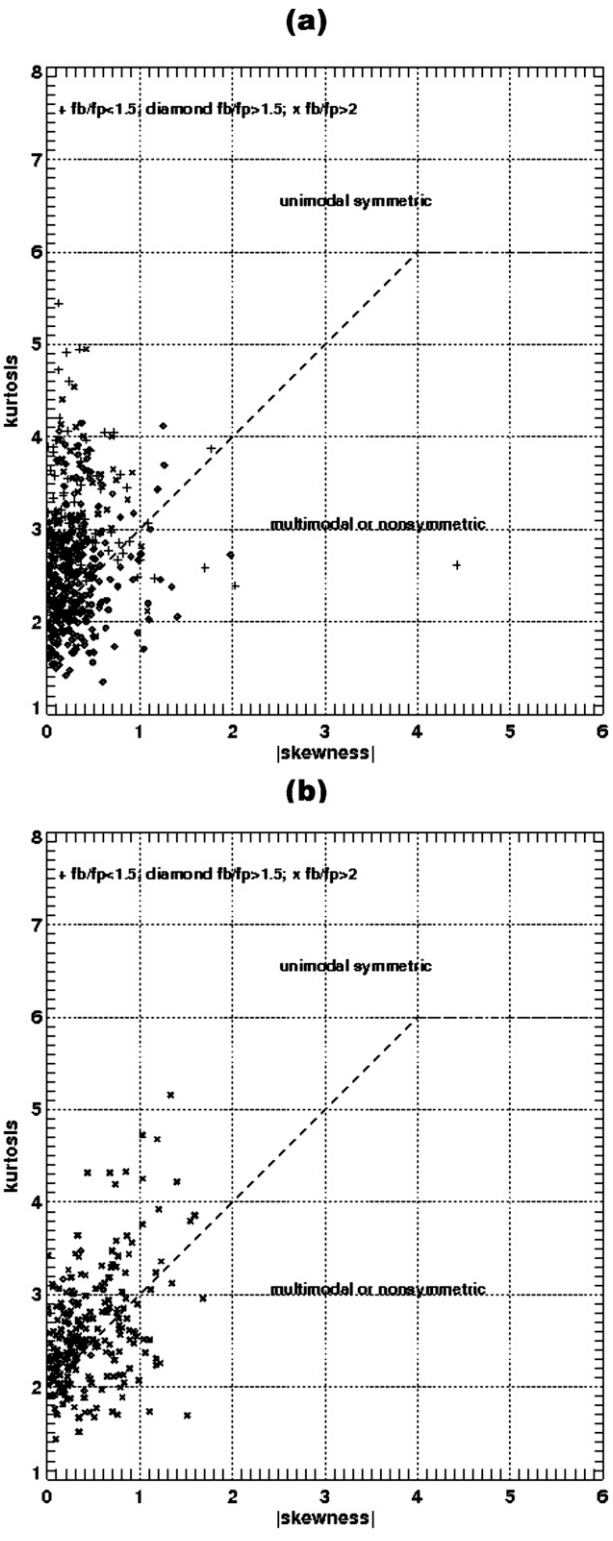

FIG. 7. Skewness–kurtosis relationships for the (a) Celtic Sea and (b) Fedje. The boundaries between unimodal and multimodal distributions (dashed line) are shown.

Segregating these data by wave age did not provide any useful additional information. Figure 9 shows the variation with direction difference for this case, and there is some indication that the departures from the dispersion relationship are associated with winds directed along the radar beam toward the radar (±180°), though again not for all cases. These are long fetch cases. Waves would be fetch limited when the winds are blowing in the opposite direction (0°; the fetch-limited range is shown on Fig. 9, see also Table 1), and therefore they are likely to have smaller values of f_b/f_p. However, some of the scatter could be attributable to difficulties in clearly identifying the first-order Bragg peaks in high sea conditions when the second-order part of the spectrum is very high in magnitude. Thus, although these results are suggestive, they are not conclusive.

If the dispersion relationship did break down when the wind was blowing toward the radar it is possible that better agreement in direction and spreading could be found at a different buoy frequency. However, the directions at these higher frequencies do not vary much with frequency and, while it was possible to find nearby buoy frequencies where the buoy and radar directions were in marginally better agreement, no evidence was found in these datasets to suggest that this occurred preferentially when the wind and radar look directions were aligned.

5. Concluding remarks

In this paper shortwave direction and spreading, inferred from the two first-order peaks in HF radar Doppler spectra, have been compared with buoy measurements at the Bragg-matched frequency over a wide range of HF radio frequencies, and good agreement has been demonstrated. This was the main objective of this paper. The agreement for shortwave direction is better than that obtained for wind direction, which has been the more common application of this measurement, because these waves are not always aligned with the wind direction, particularly in short fetch and low wind speed situations. Although the directional spreading estimates are broadly in agreement with the buoy data, there are differences that have been explored using various models of wave directionality. To do this analysis the buoy wave spectra were partitioned, and only data where the wind wave part of the spectrum was dominant were retained. The peak wind wave frequency was then used in the subsequent analysis. In the partitioning, and particularly in the calculation of wave age, the biggest uncertainty is probably in the wind speed used, and this may be the source of the differences between the data and the spreading models. Local wind data were not available in any of these experiments; in the case of Liverpool Bay

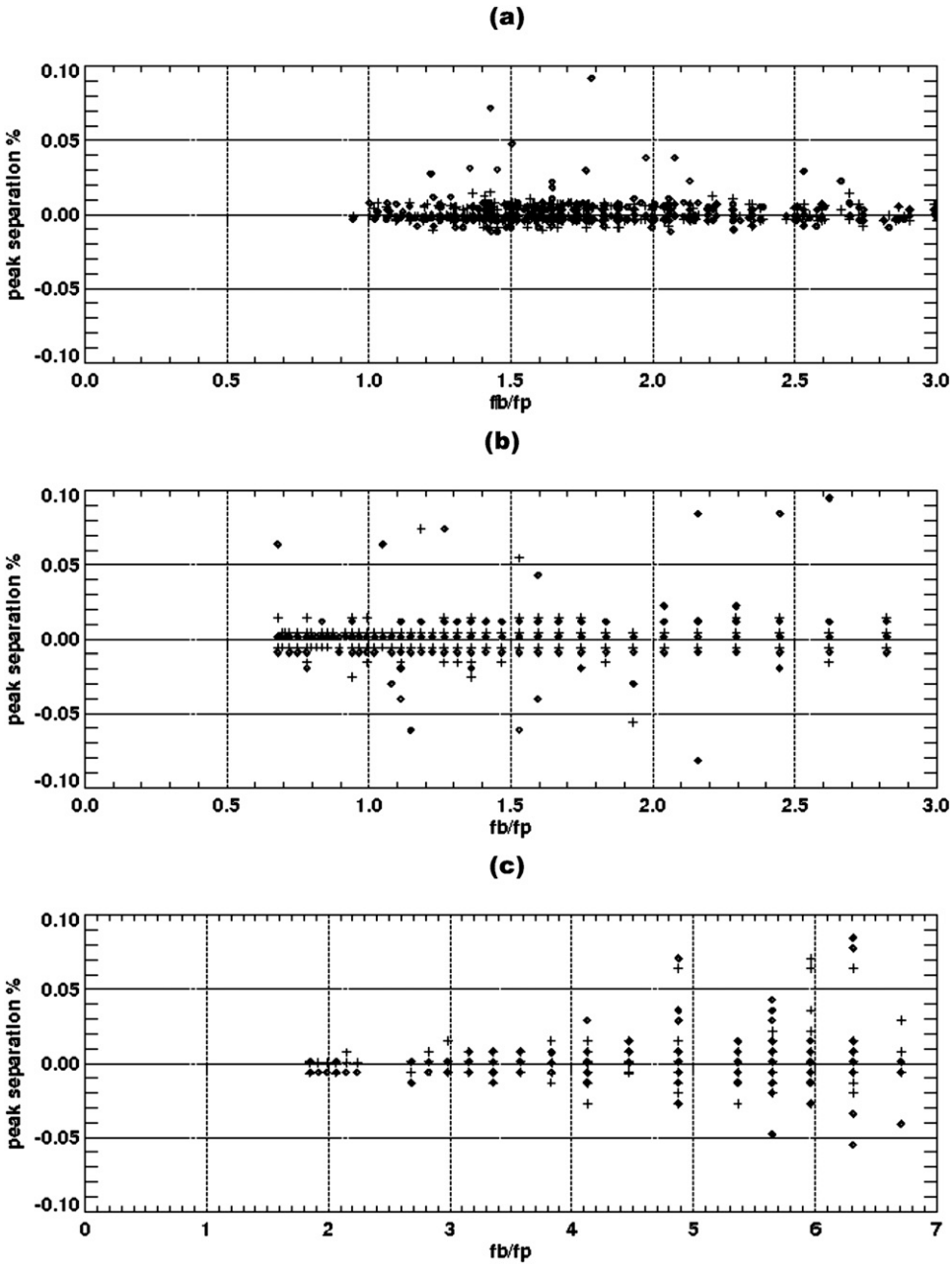

FIG. 8. Bragg peak separation plotted against Bragg-to-peak frequency for the (a) Celtic Sea, (b) Liverpool Bay, and (c) Fedje. The two symbols are for the two radars.

and Norway the wind measurements were made on the coast, and for the Celtic Sea model data were used. An analysis of HF radar data with collocated wind measurements would be a useful next step.

The method assumes a model of shortwave directionality, and the appropriateness of the model has been explored using the buoy data. The results are inconclusive, although the evidence is consistent with unimodal symmetric distributions for most of the data. However, this evidence is related to the frequency spectrum, and others have suggested that it is the wavenumber spectrum that will reveal bimodality. The radar measurement used here is of the wavenumber spectrum at a fixed (Bragg matched) wavenumber. In the comparison with the buoy data the linear dispersion relationship was used to determine which buoy frequency to use. A discussion on the evidence in the literature for a departure from the linear dispersion relationship has been

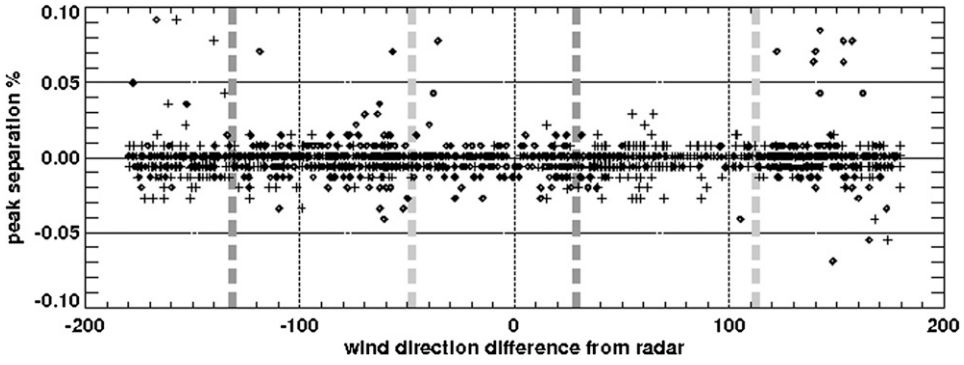

FIG. 9. Bragg peak separation plotted against difference between wind and radar beam directions for the Fedje data. The two symbols are for the two radars. The limits for fetch-limited waves for each radar (vertical dashed lines) and the radar data marked with + (darker lines).

presented and explored with these data. There is some evidence to support such a departure, at least at frequencies far from the spectral peak, but other factors—wave age, the presence of swell, high second-order returns in high seas—that could have been influencing the results have been identified. Although the potential impact of some of these has been explored, the results are inconclusive. It was not the intention of this paper to claim new insights into shortwave directionality, but the results obtained do suggest that there is scope for using HF radar in such an endeavor, although further work is needed to establish the required methodology.

In spite of the lack of conclusive evidence to support the universal use of the shortwave directional model applied here, the good comparisons between buoy and radar shortwave directions and spread suggest that it can still be used for this purpose.

Acknowledgments. The Norwegian data were obtained during the EU-funded EuroROSE project and we thank all the EuroROSE team for their contributions. The Pisces data was provided by Neptune Radar and collected during a project funded by DEFRA and the Met Office. The buoy data for this experiment have been provided by CEFAS and the model data by the Met Office. We are grateful to the radar team at POL, and the support team at Neptune Radar, for providing the Liverpool Bay radar data. The corresponding buoy data were obtained from the CEFAS Wavenet website. Some of these datasets were processed and provided by Seaview Sensing Ltd. I am grateful to the anonymous reviewers for several helpful suggestions.

REFERENCES

Akaike, H., 1974: A new look at the statistical model identification. *IEEE Trans. Automat. Contr.,* **19,** 716–723.

Apel, J. R., 1994: An improved model of the ocean surface wave vector spectrum and its effects on radar backscatter. *J. Geophys. Res.,* **99,** 16 269–16 291.

Ardhuin, F., T. H. C. Herbers, G. Ph. Van Vledder, K. P. Watts, R. Jensen, and H. C. Graber, 2007: Swell and slanting-fetch effects on wind wave growth. *J. Phys. Oceanogr.,* **37,** 908–931.

Banner, M. L., 1990: Equilibrium spectra of wind waves. *J. Phys. Oceanogr.,* **20,** 966–984.

——, and I. R. Young, 1994: Modeling spectral dissipation in the evolution of wind waves. Part I: Assessment of existing model performance. *J. Phys. Oceanogr.,* **24,** 1550–1571.

Barrick, D. E., 1972: First-order theory and analysis of MF/HF/VHF scatter from the sea. *IEEE Trans. Antennas Propag.,* **AP-20,** 2–10.

——, 1977: Extraction of wave parameters from measured HF radar sea-echo Doppler spectra. *Radio Sci.,* **12,** 415–424.

——, 1986: The role of the gravity-wave dispersion relation in HF radar measurements of the sea surface. *IEEE J. Oceanic Eng.,* **OE-11,** 285–292.

——, M. W. Evans, and B. L. Weber, 1977: Ocean surface currents mapped by radar. *Science,* **198,** 138–144.

Benoit, M., P. Frigaard, and H. A. Schaffer, 1997: Analysing multidirectional wave spectra: A tentative classification of available methods. *Proc. 1997 IAHR Conf.,* San Francisco, CA, IAHR, 131–158.

Dexter, P. E., and S. Theodorides, 1982: Surface wind speed extraction from HF sky-wave radar Doppler spectra. *Radio Sci.,* **17,** 643–652.

Donelan, M. A., J. Hamilton, and W. H. Hui, 1985: Directional spectra of wind-generated waves. *Philos. Trans. Roy. Soc. London,* **315A,** 509–562.

Elfouhaily, T., B. Chapron, K. Katsaros, and D. Vandemark, 1997: A unified directional spectrum for long and short wind-driven waves. *J. Geophys. Res.,* **102C,** 15 781–15 796.

Ewans, K. C., 1998: Observations of the directional spectrum of fetch-limited wave. *J. Phys. Oceanogr.,* **28,** 495–512.

Georges, T. M., J. A. Harlan, L. R. Meyer, and R. G. Peer, 1993: Tracking hurricane Claudette with the U.S. Air Force over-the-horizon radar. *J. Atmos. Oceanic Technol.,* **10,** 441–451.

Graber, H. C., and M. L. Heron, 1997: Wave height measurement from HF radar. *Oceanography,* **10,** 90–92.

Green, J. J., and L. R. Wyatt, 2006: Row-action inversion of the Barrick–Weber equations. *J. Atmos. Oceanic Technol.,* **23,** 501–510.

Gurgel, K.-W., G. Antonischki, H.-H. Essen, and T. Schlick, 1999: Wellen Radar (WERA): A new ground-wave HF radar for ocean remote sensing. *Coastal Eng.,* **37,** 219–234.

——, H.-H. Essen, and T. Schlick, 2006: An empirical method to derive ocean waves from second-order Bragg scattering: Prospects and limitations. *IEEE J. Oceanic Eng.,* **31,** 804–811.

Hashimoto, N., and M. Tokuda, 1999: A Bayesian approach for estimating directional spectra with HF radar. *Coastal Eng. J.,* **41,** 137–149.

Hasselmann, D. E., M. Dunckel, and J. A. Ewing, 1980: Directional wave spectra observed during JONSWAP 1973. *J. Phys. Oceanogr.,* **10,** 1264–1280.

Haus, B. K., L. K. Shay, P. A. Work, G. Voulgaris, R. J. Ramos, and J. Martinez-Pedraja, 2010: Wind speed dependence of single-site wave-height retrievals from high-frequency radars. *J. Atmos. Oceanic Technol.,* **27,** 1381–1394.

Hauser, D., K. Kahma, H. E. Krogstad, S. Lehner, J. A. J. Monbaliu, and L. R. Wyatt Eds, 2005: *Measuring and Analysing the Directional Spectra of Ocean Waves*. COST Action 714, EU Publications Office, 465 pp.

Heron, M. L., 1987: Directional spreading of short wavelength fetch-limited wind waves. *J. Phys. Oceanogr.,* **17,** 281–285.

——, P. E. Dexter, and B. T. McGann, 1985: Parameters of the air-sea interface by high-frequency ground-wave Doppler radar. *Aust. J. Mar. Freshwater Res.,* **36,** 655–670.

Hisaki, Y., 1996: Nonlinear inversion of the integral equation to estimate ocean wave spectra from HF radar. *Radio Sci.,* **31,** 25–39.

——, 2002: Short-wave directional properties in the vicinity of atmospheric and oceanic fronts. *J. Geophys. Res.,* **107,** 3188, doi:10.1029/2001JC000912.

——, 2004: Short-wave directional distribution of first-order Bragg echoes of the HF ocean radars. *J. Atmos. Oceanic Technol.,* **21,** 105–121.

——, 2007: Directional distribution of the short wave estimated from HF ocean radars. *J. Geophys. Res.,* **112,** C10014, doi:10.1029/2007JC004296.

Howarth M. J., R. J. Player, J. Wolf, and L. A. Siddons, 2007: HF radar measurements in Liverpool Bay, Irish Sea. *Proc. Oceans '07,* Aberdeen, United Kingdom, IEEE, doi:10.1109/OCEANSE.2007.4302444.

Howell, R., and J. Walsh, 1993: Measurement of ocean wave spectra using narrow beam HF radar. *IEEE J. Oceanic Eng.,* **18,** 296–305.

Kuik, A. J., G. Ph. van Vledder, and L. H. Holthuijsen, 1988: A method for the routine analysis of pitch-and-roll buoy wave data. *J. Phys. Oceanogr.,* **18,** 1020–1034.

LeBlond, P. H., 1986: Is it valid to use the linear gravity-wave dispersion relation when interpreting HF radar measurements? *IEEE J. Oceanic Eng.,* **OE-11,** 285.

Lipa, B. J., 1977: Derivation of directional ocean-wave spectra by inversion of second order radar echoes. *Radio Sci.,* **12,** 425–434.

——, and D. E. Barrick, 1986: Extraction of sea state from HF radar sea echo: Mathematical theory and modelling. *Radio Sci.,* **21,** 81–100.

Long, A. E., and D. B. Trizna, 1973: Mapping of North Atlantic winds by HF radar sea backscatter interpretation. *IEEE Trans. Antennas Propag.,* **21,** 680–685.

Longuet-Higgins, M. S., 1976: On the nonlinear transfer of energy in the peak of a gravity-wave spectrum: A simplified model. *Proc. Roy. Soc. London,* **347A,** 311–328.

Lygre, A., and H. E. Krogstad, 1986: Maximum entropy estimation of the directional distribution in ocean wave spectra. *J. Phys. Oceanogr.,* **16,** 2052–2060.

Maresca, J. W., and T. M. Georges, 1980: Measuring rms wave-height and the scalar ocean wave spectrum with HF skywave radar. *J. Geophys. Res.,* **85C,** 2759–2771.

Mitsuyasu, H., F. Tasai, T. Suhara, S. Mizuno, M. Ohkusu, T. Honda, and K. Rikiishi, 1975: Observations of the directional spectrum of ocean waves using a cloverleaf buoy. *J. Phys. Oceanogr.,* **5,** 750–760.

Phillips, O. M., 1981: The dispersion of short wavelets in the presence of a dominant long wave. *J. Fluid Mech.,* **107,** 465–485.

Robinson, A. M., L. R. Wyatt, and M. J. Howarth, 2011: A two year comparison between HF radar and ADCP current measurements in Liverpool Bay. *J. Oper. Oceanogr.,* **4,** 33–45.

Stewart, R. H., and J. W. Joy, 1974: HF radio measurements of surface currents. *Deep-Sea Res.,* **21,** 1039–1049.

——, and J. R. Barnum, 1975: Radio measurements of oceanic winds at long ranges: An evaluation. *Radio Sci.,* **10,** 853–857.

Toffoli, A., M. Onorato, E. M. Bitner-Gregersen, and J. Monbaliu, 2010: Development of a bimodal structure in ocean wave spectra. *J. Geophys. Res.,* **115,** C03006, doi:10.1029/2009JC005495.

Tucker, M. J., and E. G. Pitt, 2001: *Waves in Ocean Engineering*. Elsevier Ocean Engineering Book Series, Vol. 5, Elsevier, 548 pp.

Tyler, G. L., C. C. Teague, R. H. Stewart, A. M. Peterson, W. H. Munk, and J. W. Joy, 1974: Wave directional spectra from synthetic aperture observations of radio scatter. *Deep-Sea Res.,* **21,** 989–1016.

Vesecky, J. F., J. Drake, C. C. Teague, F. L. Ludwig, K. Davidson, and J. Paduan, 2002: Measurement of wind speed and direction using multifreqeuency HF radar. *Proc. IGARSS'02,* Vol. 3, Toronto, ON, Canada, IEEE, 1899–1901.

Voorrips, A. C., V. K. Makin, and S. Hasselmann, 1997: Assimilation of wave spectra pitch-and-roll buoys in a North Sea wave model. *J. Geophys. Res.,* **102C,** 5829–5849.

Wyatt, L. R., 1988: Significant wave height measurement with HF radar. *Int. J. Remote Sens.,* **9,** 1087–1095.

——, 1990: A relaxation method for integral inversion applied to HF radar measurement of the ocean wave directional spectrum. *Int. J. Remote Sens.,* **11,** 1481–1494.

——, 1999: HF radar measurements of the development of the directional wave spectrum. *The Wind-Driven Air-Sea Interface: Electromagnetic and Acoustic Sensing, Wave Dynamics and Turbulent Fluxes,* M. L. Banner, Ed., School of Mathematics, University of New South Wales, 433–440.

——, 2000: Limits to the inversion of HF radar backscatter for ocean wave measurement. *J. Atmos. Oceanic Technol.,* **17,** 1651–1666.

——, 2002: An evaluation of wave parameters measured using a single HF radar system. *Can. J. Remote Sens.,* **28,** 205–218.

——, L. J. Ledgard, and C. W. Anderson, 1997: Maximum likelihood estimation of the directional distribution of 0.53-Hz ocean waves. *J. Atmos. Oceanic Technol.,* **14,** 591–603.

——, and Coauthors, 2003: Validation and intercomparisons of wave measurements and models during the EuroROSE experiments. *Coastal Eng.,* **48,** 1–28.

——, J. J. Green, A. Middleditch, M. D. Moorhead, J. Howarth, M. Holt, and S. Keogh, 2006: Operational wave, current and wind measurements with the Pisces HF radar. *IEEE J. Oceanic Eng.,* **31,** 819–834.

——, ——, and ——, 2011: HF radar data quality requirements for wave measurement. *Coastal Eng.,* **58,** 327–336.

Young, I. R., 2010: The form of the asymptotic depth-limited wind wave spectrum: Part III—Directional spreading. *Coastal Eng.,* **57,** 30–40.

Zhang, F. W., W. M. Drennan, B. K. Haus, and H. C. Graber, 2009: On wind-wave-current interactions during the Shoaling Waves Experiment. *J. Geophys. Res.,* **114,** C01018, doi:10.1029/2008JC004998.